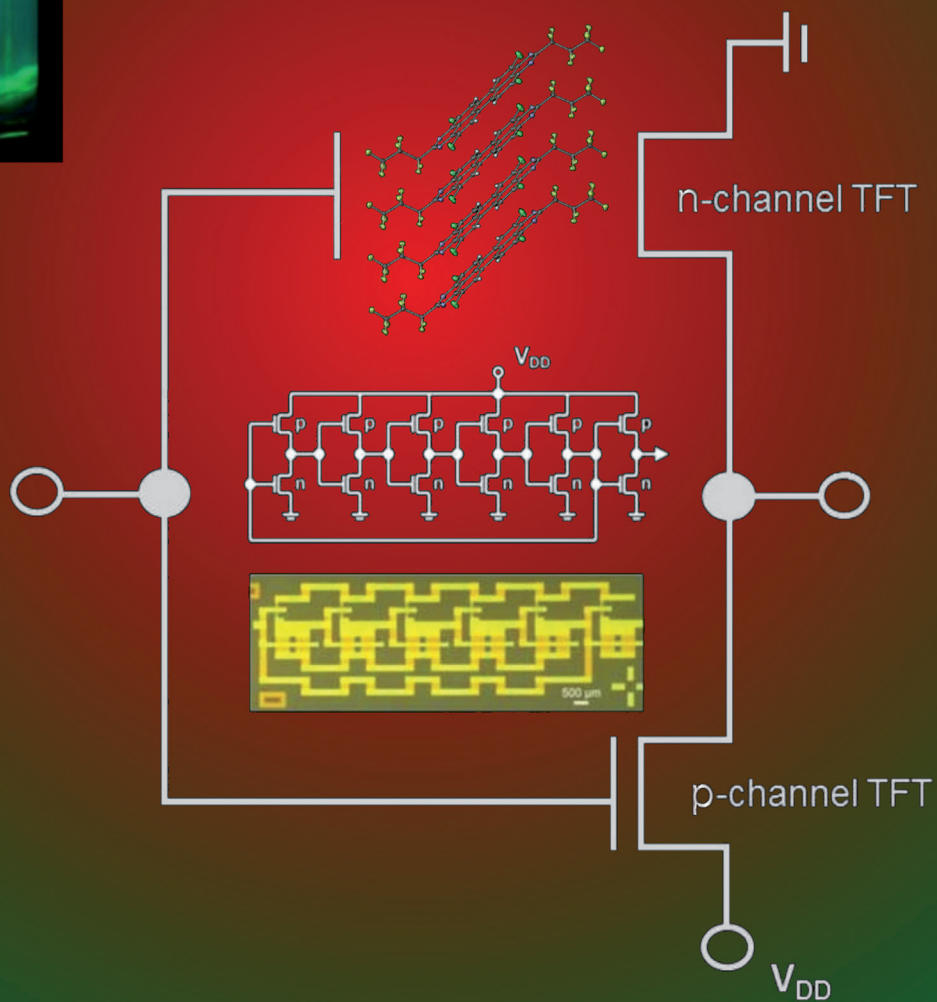
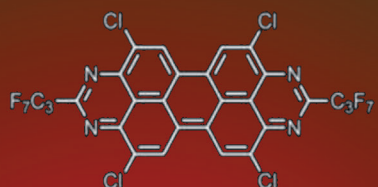
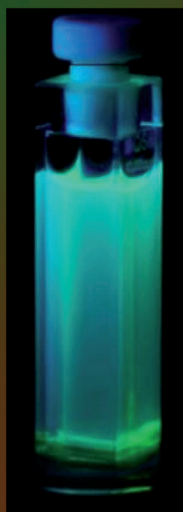




Tetrachlorinated Tetraazaperopyrenes (TAPPs): Highly Fluorescent Dyes and Semiconductors for Air-Stable Organic n-Channel Transistors and Complementary Circuits

Susanne C. Martens,^[a] Ute Zschieschang,^[b] Hubert Wadebold,^[a] Hagen Klauk,^[b] and Lutz H. Gade*^[a]

Organic Electronics with Tetraazaperopyrenes



Abstract: A range of 2,9-perfluoroalkyl-substituted tetraazaperopyrene (TAPP) derivatives (**1–5**) was synthesised by reacting 4,9-diamino-3,10-perylenequinone diimine (DPDI) with the corresponding carboxylic acid chloride or anhydride in the presence of a base. The reaction of compounds **1–4** with dichloroisocyanuric acid (DIC) in concentrated sulphuric acid resulted in the fourfold substitution of the tetraazaperopyrene core, yielding the 2,9-bisperfluoroalkyl-4,7,11,14-tetrachloro-1,3,8,10-tetraazaperopyrenes **6–9**, respectively. The optical and electrochemical data demonstrate the drastic

influence of the core substitution on the properties. All compounds are highly luminescent (fluorescence quantum yields of up to $\Phi=0.8$). The LUMO energies of the tetrachlorinated TAPP derivatives (determined by cyclic voltammetry and computed by DFT calculations) were found to be below -4 eV . In the course of this work the performance of TAPP deriva-

tives in organic thin-film transistors (TFTs) was investigated, and their n-channel characteristics with field-effect mobilities of up to $0.14\text{ cm}^2\text{ V}^{-1}\text{ s}^{-1}$ and an on/off current ratio of $>10^6$ were confirmed. Long-term stabilities of 3–4 months under ambient conditions of the devices were established. Complementary inverters and ring oscillators with n-channel TFTs based on compound **8** and p-channel TFTs based on dinaphtho-[2,3-b:2',3'-f]thieno[3,2-b]thiophene (DNTT) were fabricated on a glass substrate.

Keywords: azaaromatics • fluorescence • organic electronics • organic semiconductors • thin-film transistors

Introduction

Organic semiconductors are key components of numerous electronic and optoelectronic devices for a wide range of applications, such as light-emitting diodes, photovoltaic cells and organic thin-film transistors (TFTs). Thus the search for new organic materials that serve this purpose is of considerable current interest.^[1–6] To date most efforts have been devoted to the development of organic semiconductors with p-type characteristics, whereas n-channel materials came into the focus of research more recently. So far the performance of organic p-type semiconductors outmatches the known n-type materials by far.^[5,7] Nevertheless, the availability of both kinds of semiconducting materials is necessary for the fabrication of complementary integrated circuits, bipolar transistors or organic p/n junctions.^[1–6,8] Therefore the development of organic n-channel materials with both high mobility and, in particular, good stability in air remains a challenge.

Most single-molecule organic semiconductors are composed of extended π -conjugated systems. The incorporation of heteroatoms into the aromatic framework of polycyclic aromatic hydrocarbons (PAHs) is a commonly used methodology to improve their charge-carrier characteristics for applications in organic electronics.^[9,10] The current strategy to obtain air-stable n-type semiconductors is to reduce the orbital energies of their lowest unoccupied molecular orbitals (LUMOs) by introducing strong electron-withdrawing substituents onto the π -conjugated system. This reduces their susceptibility to oxidation and the ease of electron injection from air-stable, high-workfunction contacts.^[6,10–12]

Several years ago, we developed an efficient, metal-induced synthesis of 4,9-diamino-3,10-perylenequinone diimine (DPDI) by oxidative coupling of two 1,8-diaminonaphthalene units.^[13,14] This functionalised perylene may be converted into a tetraazaperopyrene (TAPP) and a range of derivatives, which are potentially interesting materials for the application in organic electronic devices. The preparation of these materials is accomplished by treating DPDI with triethyl orthoformate in the presence of catalytic amounts of formic acid yielding the parent compound TAPP^[15,16] or with carboxylic acid chlorides or anhydrides leading to the formation of the corresponding 2,9-disubstituted derivatives.

Here we present a detailed study of the optical and redox properties of new 2,9-perfluoroalkyl-substituted tetraazaperopyrenes. Perfluorinated alkyl groups have proven to act as qualified electron-withdrawing groups to significantly lower the LUMO energies and improve the ability of a material to act as an n-channel organic semiconductor. In addition to this, perfluorinated alkyl groups seem to have a positive, so far not completely understood, packing effect that leads to a significant increase of the air stability of organic n-channel semiconductors.^[10,11a–b,17,18] Furthermore, for the first time, we were able to functionalise TAPPs by core substitution, opening up new possibilities of controlling the optical and redox properties of this class of functional dyes and thus widening the scope of applications. In the course of this work, we investigated the performance of the compounds presented herein as organic semiconductors in n-channel thin-film transistors (TFTs) and their integration into organic electronic circuits. To the best of our knowledge, this is the first time that tetraazaperopyrenes have been employed in organic transistors.

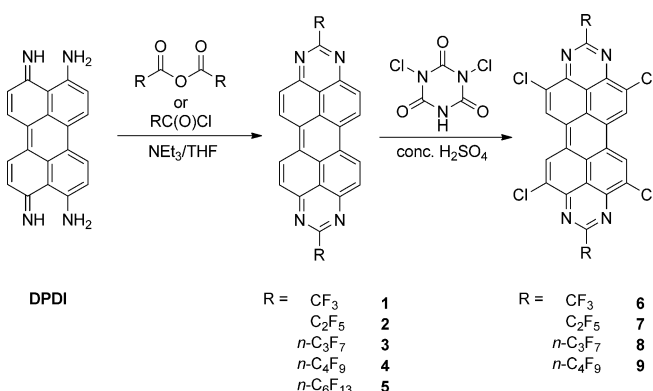
[a] Dr. S. C. Martens, Prof. Dr. H. Wadeohl, Prof. Dr. L. H. Gade
Anorganisch-Chemisches Institut, Universität Heidelberg
Im Neuenheimer Feld 270, 69120 Heidelberg (Germany)
Fax: (+49) 6221545609
E-mail: lutz.gade@uni-hd.de

[b] Dr. U. Zschieschang, Dr. H. Klauk
Max Planck Institute for Solid Research
Heisenbergstr. 1, 70569 Stuttgart (Germany)

 Supporting information for this article is available on the WWW under <http://dx.doi.org/10.1002/chem.201103158>.

Results and Discussion

Synthesis of 2,9-bisperfluoroalkyl-1,3,8,10-tetraazaperopyrenes and their core-chlorinated derivatives: The synthesis of 2,9-bisperfluoroalkyl-1,3,8,10-tetraazaperopyrene (**1–5**) was achieved by reacting DPDI either with the corresponding carboxylic acid chloride or anhydride (2.5 mol equiv) in the presence of triethylamine in THF (Scheme 1). Purification



Scheme 1. Synthesis of the 2,9-bis-perfluoroalkyl-substituted TAPP derivatives **1–5** and their corresponding core-chlorinated derivatives **6–9**.

was accomplished by sublimation at 440 °C in a weak stream of nitrogen. Reaction of compounds **1–4** with dichloroisocyanuric acid (DIC) in concentrated sulphuric acid led to the fourfold substitution of the tetraazaperopyrene core, yielding the 2,9-bisperfluoroalkyl-4,7,11,14-tetrachloro-1,3,8,10-tetraazaperopyrenes **6–9**, respectively (Scheme 1), which were purified by recrystallisation from THF. All compounds were fully characterised by elemental analysis, high-resolution mass spectrometry and ¹H, ¹³C and ¹⁹F NMR spectroscopy.

Whereas the study of the properties of previously described TAPP derivatives was often limited by their lack of solubility in common organic solvents,^[15,20] compounds **2–5** were found to be sufficiently soluble in polar organic solvents for the study of their redox chemistry and photophysics. Moreover, the introduction of additional substituents at the TAPP core led to a drastic increase of solubility, enhancing the viable concentration for example, in THF from about 10⁻⁶ M up to approximately 10⁻² M.

Crystal structures: Crystals of compound **3** suitable for X-ray diffraction were grown by sublimation at 440 °C in a horizontal glass tube in a weak stream of nitrogen. Crystals of the core-substituted derivatives **7** and **8** suitable for X-ray diffraction were grown from chlorobenzene and THF, respectively. All three compounds crystallise in the triclinic space group $P\bar{1}$ and the solid-state structures show crystallographic C_i molecular symmetry. Their molecular structures are determined by the almost planar tetraazaperopyrene core with nearly identical bond lengths and angles and the two perfluoroalkyl substituents pointing in opposite direc-

tions above and below the tetraazaperopyrene core. The chlorinated derivatives possess a slightly more twisted structure than compound **3**, which is probably caused by steric repulsion of the chlorine substituents (Table 1). As an example, the top and side view of **3** are shown in Figure 1 along with selected bond lengths.

Table 1. Selected details of crystal structures of compounds **3**, **7** and **8**.

	3	7	8
crystal system	triclinic	triclinic	triclinic
space group	$P\bar{1}$	$P\bar{1}$	$P\bar{1}$
$\pi-\pi$ plane distance [Å]	3.51	3.37	3.38
torsion angle ^[a]	-0.4(4)	-1.4(5)	-1.4(3)
torsion angle (DFT) ^[b]	-0.30	-0.30	-0.29

[a] Torsion angle between the two connected naphthalene units C3-C4-C10'-C9'. [b] Calculated at the B3PW91/6-31 g(d,p) level of theory.

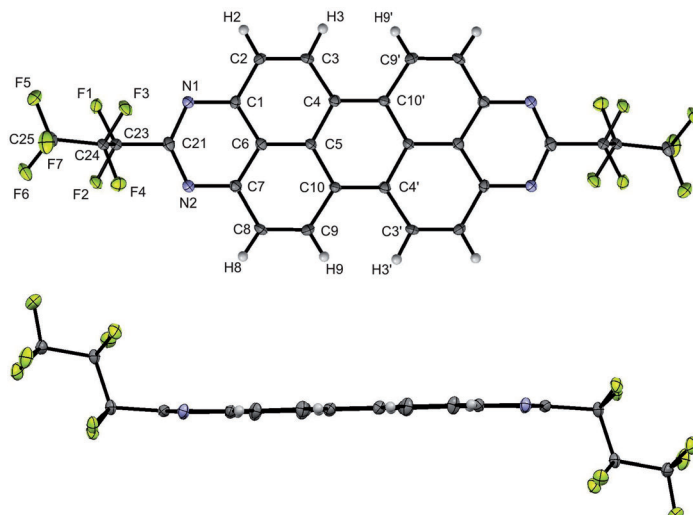


Figure 1. Molecular structure of **3**: top view (top) and side view (bottom). Thermal ellipsoids were drawn at the 50% probability level. Principal bond lengths [Å]: C23–C21 1.526(3), C21–N1 1.329(3), C1–N1 1.350(3), C7–N2 1.348(3), C1–C2 1.426(3), C2–C3 1.354(3), C3–C4 1.435(3), C4–C5 1.425(3), C4–C10' 1.416(3), C5–C6 1.424(3), C6–C7 1.411(3), C7–C8 1.425(3), C8–C9 1.351(3), C9–C10 1.445(3).

The intermolecular packing pattern of all compounds is characterised by a slip-stacked face-to-face arrangement (Figure 2) with a short interplanar distance of 3.37–3.51 Å. We note that for the core-substituted derivatives **7** and **8** the interplanar distance between neighbouring molecules within a column is smaller (3.37 Å) than in the case of derivative **3** (3.51 Å). Both values are still in good accordance with the range of 3.34–3.55 Å previously established for perylene bisimides.^[19]

Characteristics as chromophores and fluorophores: All of the 2,9-bisperfluoroalkyl substituted derivatives **1–5** are yellow in the solid state as well as in solution. With the exception of compound **1**, the solubility of these derivatives (**2–5**) is significantly greater than that of their non-fluorinat-

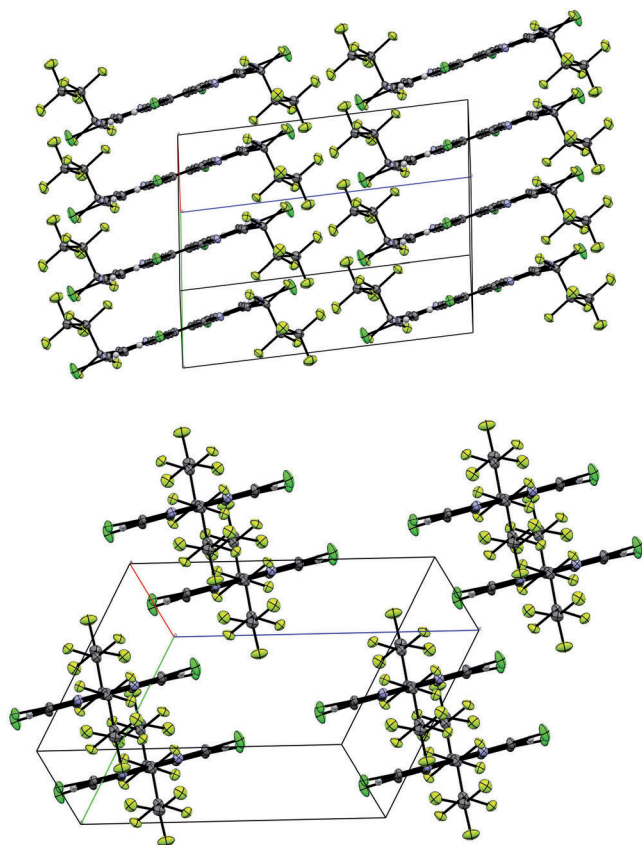


Figure 2. Packing of the molecules of **8** in the crystal form showing the slip-stacked face-to-face arrangement from two different views.

ed analogues, which allowed a systematic study of their optical properties in THF. As observed for the UV/Vis absorption spectra of the previously published TAPP derivatives recorded in concentrated acids,^[15,20] the UV/Vis absorption spectra of compounds **1–5** recorded in neat THF are almost superimposable. They display a characteristic visible absorption band with a maximum at 436 nm ($\log \epsilon = 4.50\text{--}4.80$, Table 2). The band is characterised by a strong vibrational progression of about 1450 cm^{-1} , typical for $\pi^*\leftarrow\pi$ transitions in polycondensed aromatics and, in particular, for perylene derivatives. The absence of a significant effect of the substituents in the 2- and 9-positions on the absorption spectra

Table 2. $\pi^*\leftarrow\pi$ Transition λ_{\max} [nm] and vibrational progression $\Delta\nu$ [cm^{-1}] in the absorption and emission spectra recorded in THF.

	λ_{\max} [nm] ($\log \epsilon$)	$\Delta\nu$ [cm^{-1}]	λ_{em} [nm] (Stokes Shift)	ϕ_{em}	τ [ns]
1	436 (− ^a)	1454	445 (9)	0.30	2.53
2	436 (4.50)	1401	446 (10)	0.53	2.37
3	436 (4.70)	1454	448 (12)	0.51	2.44
4	436 (4.74)	1454	445 (9)	0.53	2.49
5	436 (4.80)	1454	445 (9)	0.55	2.51
6	469 (4.80)	1457	479 (10)	0.78	2.38
7	469 (4.91)	1509	480 (13)	0.80	2.33
8	469 (4.89)	1405	479 (10)	0.78	2.34
9	468 (4.77)	1412	479 (11)	0.81	2.34

[a] Compound was not completely dissolved.

indicates that their influence on the HOMO–LUMO gap of the tetraazaperopyrene core is negligible; we attribute this result to the fact that the frontier orbitals of the TAPPs exhibit a nodal plane running along their long molecular axis and therefore passing through the carbon atoms C2 and C9.^[15,20]

As expected, the emission spectra image the mirror symmetry of the absorbance spectra with Stokes shifts of about 10 nm (Figure 3 top). The fluorescence spectra of compounds **1–5** recorded in THF are characterised by an emission band with a maximum at 446 nm with the characteristic vibrational progression (Table 2). The perfluoroalkyl substituents have a remarkable effect on the emission characteristics of the TAPPs: Whilst the luminescence quantum yields of the previously known TAPP derivatives in organic solvents did not exceed 0.01, the corresponding values of the 2,9-bisperfluoroalkyl-substituted TAPPs in THF are significantly increased, ranging from 0.30 (**1**) to 0.50 (**2–5**). This remarkable enhancement is probably due to the reduced tendency to form aggregates in solution.

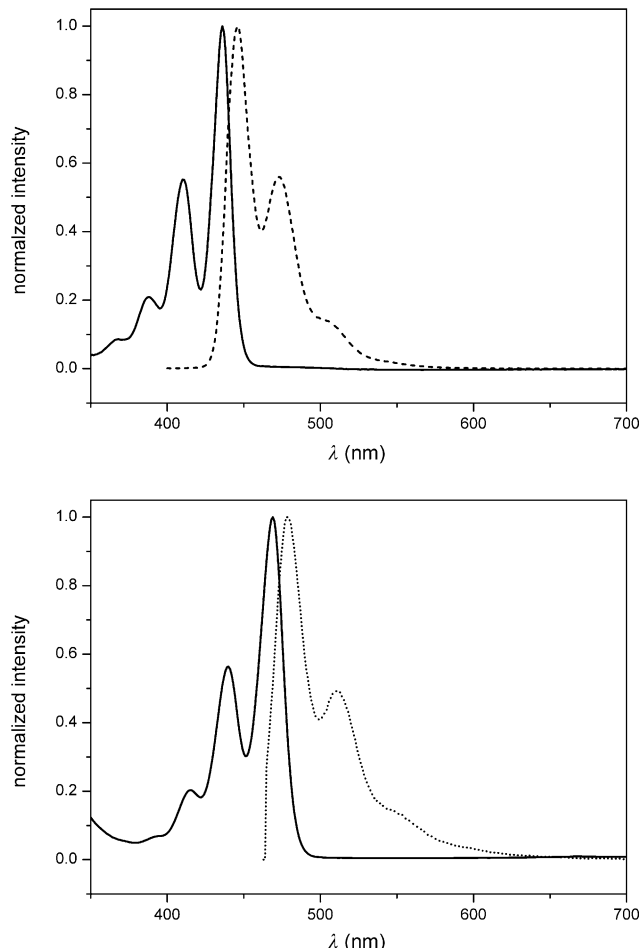


Figure 3. Top: normalised UV/Vis absorption (solid line) and emission (dashed line) spectra of compound **3**; bottom: normalised UV/Vis absorption (solid line) and emission (dotted line) spectra of compound **8** recorded in THF.

On the other hand, substitution of the tetraazaperopyrene core leads to a drastic change of the absorption properties, because this affects the frontier orbitals to a different degree (*vide infra*). In this case, the HOMO–LUMO gap is significantly altered. The core-substituted derivatives **6–9** are yellow to red in the solid state and their colour in solution is strongly dependent on the concentration, ranging from bright yellow to deep orange to red. As for the compounds discussed above, the UV/Vis absorption spectra of derivatives **6–9** in THF are almost superimposable. Compared to **1–5**, their absorption band is significantly shifted to greater wavelengths, displaying a maximum at 469 nm ($\log \epsilon = 4.70\text{--}4.90$; Table 2) as well as a strong vibrational progression of about 1400 cm^{-1} (Figure 3 bottom).

As in the case of **1–5**, the emission spectra of **6–9** show the characteristic mirror image of the absorption spectra (Figure 3 bottom) with Stokes shifts of about 10 nm and a maximum at 479 nm with the characteristic vibrational progression (Table 2). The introduction of the chlorine substituents not only leads to a significant bathochromic shift of the absorption and emission bands, but also results in an increase of the luminescence quantum yields ($\Phi_{\text{Em}}(\mathbf{2})=0.50$ compared to $\Phi_{\text{Em}}(\mathbf{7})=0.80$; Table 2).

Electronic structures of the TAPP derivatives: For the determination of the predominant type of charge carriers in an organic material as well as for their stability in typical organic semiconductors, the knowledge of the relative HOMO and LUMO energetic positions is crucial. In the case of organic n-type materials, in which the charge transport occurs predominantly by hopping through low-lying LUMOs, energies of less than -3.8 eV are required for an efficient electron injection into the semiconductor according to the literature.^[11c,17,21] Furthermore, the lower the LUMO energy, the lower is the bias required for injection of the charge carriers and the less susceptible are the electrons to trapping.

The electronic properties of the new TAPP derivatives were experimentally characterised by cyclic voltammetry (CV) and UV/Vis absorption spectroscopy (*vide supra*). Furthermore, DFT calculations were performed to investigate the frontier molecular orbital energies. The ground-state geometries of all TAPP derivatives were optimised at the B3PW91/6-31 g(d,p) level of theory, followed by frequency analyses to verify the energy minima. In general, the optimised structures were in good agreement with the metric parameters of the crystallographically characterised TAPP derivatives.

The calculated (gas-phase) LUMO energies as well as the data derived from cyclic voltammetry^[22] are summarised in Table 3. The cyclic voltammograms of the non-chlorinated TAPP derivative **5** (Figure 4 a) and of the chlorinated congener **8** (Figure 4 b), recorded in THF, illustrate the influence of the core substitution on the redox behaviour of tetraazaperopyrenes. In all cases, the experimentally determined values (CV) and the orbital energies calculated by DFT are in excellent agreement, indicating that the chosen computational method is suitable for the prediction of the electronic

Table 3. Cyclovoltammetric data, LUMO energies and electron affinities for compounds **1–9**.

	E_{Red1} [V] ^[a]	E_{Red2} [V] ^[a]	E_{LUMO} [eV] ^[b]	E_{LUMO} [eV] ^[c]	EA [eV] ^[c]
1	–	–	–	–3.66	2.46
2	−0.53	−0.95	−3.72	−3.68	2.51
3	−0.53	−0.96	−3.72	−3.70	2.53
4	−0.50	−0.92	−3.72	−3.71	2.55
5	−0.53	−0.96	−3.72	−3.72	2.57
6	−0.22	−0.61	−4.02	−4.11	3.01
7	−0.22	−0.62	−4.03	−4.14	3.05
8	−0.18	−0.59	−4.06	−4.14	3.07
9	−0.21	−0.61	−4.03	−4.14	3.08

[a] Measured against SCE in THF. [b] Determined according to literature methods using Fc/Fc⁺ as an internal standard ($E_{\text{HOMO}}(\text{Fc})=-4.8\text{ eV}$).^[22]
[c] Calculated at the B3PW91/6-31 g(d,p) level of theory.

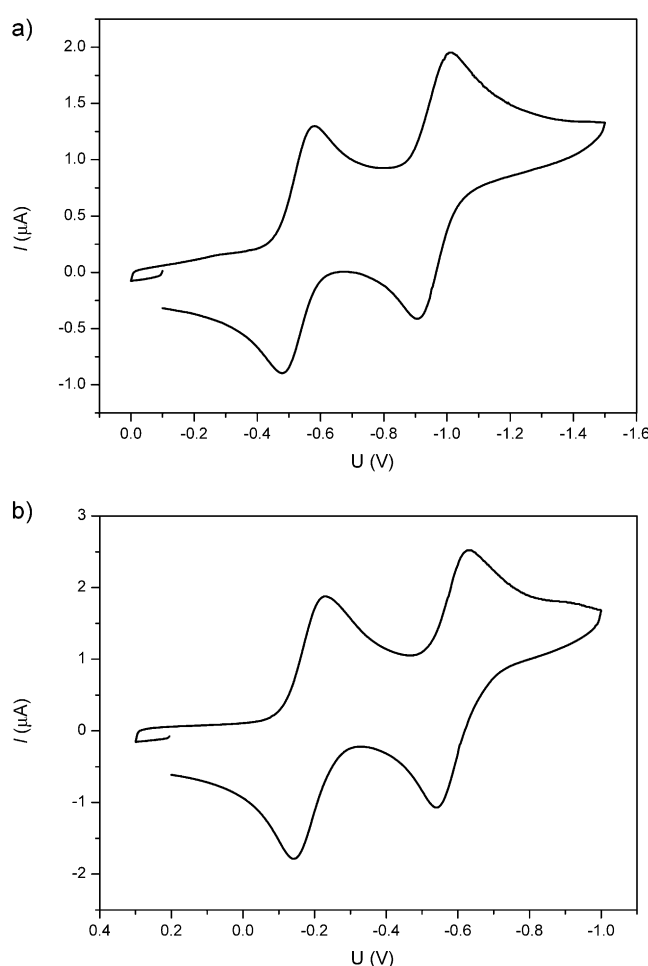


Figure 4. Cyclic voltammogram of a) **5** and b) **8** recorded in THF (sweep rate 50 mV s^{-1} , supporting electrolyte Bu_4NPF_6 , reference SCE).

properties of TAPP derivatives. As already discussed above, it is not possible to change the HOMO–LUMO gap of these compounds significantly by variation of the substituents in the 2- and 9-positions, owing to the fact that their frontier orbitals exhibit a nodal plane that runs through the substituted carbon atoms.^[20] However, the frontier molecular orbital energies themselves are influenced, as illustrated by com-

parison of the experimentally determined LUMO energy of **4** (-3.72 eV) with the corresponding value of its non-fluorinated analogue 2,9-di-*n*-butyl-TAPP^[23] (-3.38 eV). As expected, the introduction of electron-withdrawing groups leads to a significant lowering of the LUMO energies which for the 2,9-perfluoroalkyl-substituted TAPP derivatives come close to the range that is desirable for organic n-channel TFTs (vide supra).

In the same way as the LUMO energies were lowered, the calculated electron affinities (EAs) increased by changing the substituent from alkyl to perfluoroalkyl (for example: 2,9-di-*n*-butyl-TAPP: 2.37 eV; **4**: 2.55 eV). EAs serve as a second indicator determining the suitability of an organic material as an organic semiconductor. Chao et al. have recently elucidated the correlation between ambient stability of known n-type semiconductors and the adiabatic electron affinity of the organic molecule and derived a threshold value of 2.8 eV to provide the stability of the radical anion species against ambient oxidants, such as water and oxygen.^[24] The EAs of the derivatives discussed herein (Table 3) were calculated by optimising the structure of the anionic species, using the previously optimised geometry of the neutral species as a starting point and taking the difference of the total energies of both species. It is evident that the influence of the electron-withdrawing perfluoroalkyl groups is too small to lead to a sufficient increase of the EAs as well as a sufficient decrease of the LUMO energies for the application of these molecules as organic n-type semiconducting materials. However, the introduction of additional electron-withdrawing groups, such as the four chlorine substituents in **6–9**, led to a further decrease of the LUMO energies as well as a sufficient increase of the EAs (Table 3). For all four chlorinated derivatives **6–9** the LUMO energies and EAs lie in the above-mentioned target area for potential n-type organic semiconductors.

Electron mobility of the TAPPs in thin-film transistors: The potential of the TAPPs for transistor applications was evaluated in bottom-gate, top-contact TFTs and complementary circuits. In one type of TFT, the substrate was a doped Si wafer (also serving as the gate electrode) and the gate dielectric a combination of 100 nm thick SiO_2 (grown by thermal oxidation), 8 nm thick AlO_x (deposited by atomic layer

deposition), and a 1.7 nm thick self-assembled monolayer (SAM) of tetradecylphosphonic acid. We note that high-quality aliphatic SAMs often enhance the morphology of the organic semiconductor layer, and since alkylphosphonic acids form high-quality SAMs on AlO_x but not on SiO_2 ,^[25] the SiO_2 layer was first covered with AlO_x . In the second type of TFT, the substrate was either Si or glass, the gate electrode 20 nm thick Al (deposited by evaporation through a shadow mask), and the gate dielectric a combination of 3.6 nm thick AlO_x (grown by plasma oxidation) and a 1.7 nm thick SAM of tetradecylphosphonic acid. A 20 – 30 nm thick layer of the corresponding TAPP derivative was vacuum-deposited onto the gate dielectric, and Au source/drain contacts were deposited on top of the semiconductor by evaporation through a shadow mask. All measurements were carried out in air.

In n-channel TFTs, a positive gate-source voltage induces accumulation of electrons in the semiconductor near the dielectric interface and thereby a positive drain current. The TFT parameters electron mobility (μ_n), on/off current ratio ($I_{\text{on}}/I_{\text{off}}$), threshold voltage (V_{th}) and subthreshold swing (SS) were extracted from the current–voltage characteristics.^[26] The mobility was determined in the saturation regime.

All TFTs exclusively display n-channel characteristics and can be operated in air. The TFT parameters are summarised in Table 4. For each compound, the optimum substrate temperature was independently determined. The best performance was obtained with the heptafluoropropyl-substituted core-chlorinated derivative **8** deposited onto substrates held at a temperature of 90°C . In this case an electron mobility of $0.14 \text{ cm}^2 \text{ V}^{-1} \text{ s}^{-1}$ was measured for TFTs on Si substrates with a thick $\text{SiO}_2/\text{AlO}_x/\text{SAM}$ gate dielectric, and an electron mobility of $0.035 \text{ cm}^2 \text{ V}^{-1} \text{ s}^{-1}$ for TFTs on glass substrates with a thin AlO_x/SAM gate dielectric (see Figure 5). Shelf-life tests indicate that TFTs based on **8** have excellent stability in air even over periods of 3–4 months.

It is interesting to note, that for both the core-substituted TAPPs (**7–9**) and the derivatives without core substituents (**2–5**), the maximum electron mobility was measured for the molecules with the heptafluoropropyl substituents (**3** and **8**). A similar observation was recently reported by Schmidt et al. for perylene tetracarboxylic diimides (PTCDIs) with fluoroalkyl substituents ranging in length from two to five

Table 4. Summary of the transistor parameters electron field-effect mobility (μ_n), on/off current ratio ($I_{\text{on}}/I_{\text{off}}$), threshold voltage (V_{th}) and subthreshold swing (SS) measured in ambient air.

	TFTs with thick $\text{SiO}_2/\text{AlO}_x/\text{SAM}$ gate dielectric				T [$^\circ\text{C}$] ^[a]	TFTs with thin AlO_x/SAM gate dielectric				T [$^\circ\text{C}$] ^[a]
	μ_n [$\text{cm}^2 \text{ V}^{-1} \text{ s}^{-1}$]	$I_{\text{on}}/I_{\text{off}}$	V_{th} [V]	SS [V decade $^{-1}$]		μ_n [$\text{cm}^2 \text{ V}^{-1} \text{ s}^{-1}$]	$I_{\text{on}}/I_{\text{off}}$	V_{th} [V]	SS [V decade $^{-1}$]	
1	0.04	10^6	29	1.6	70	0.01	10^2	2.2	0.28	70
2	0.03	10^5	32	3.0	70	0.01	10^4	2.0	0.26	70
3	0.05	10^5	29	2.0	100	0.03	10^3	2.1	0.27	100
4	0.01	10^4	34	2.3	70	0.03	10^3	1.6	0.20	100
5	0.002	10^4	36	3.3	90	0.005	10^3	1.9	0.37	100
6	0.01	10^4	22	2.6	70	0.001	10^3	1.2	0.42	70
7	0.01	10^5	25	2.4	70	0.015	10^4	1.7	0.25	70
8	0.14	10^6	22	2.0	90	0.035	10^5	1.7	0.25	90
9	0.005	10^5	20	3.6	100	0.005	10^3	1.2	0.31	100

[a] Substrate temperature during semiconductor deposition.

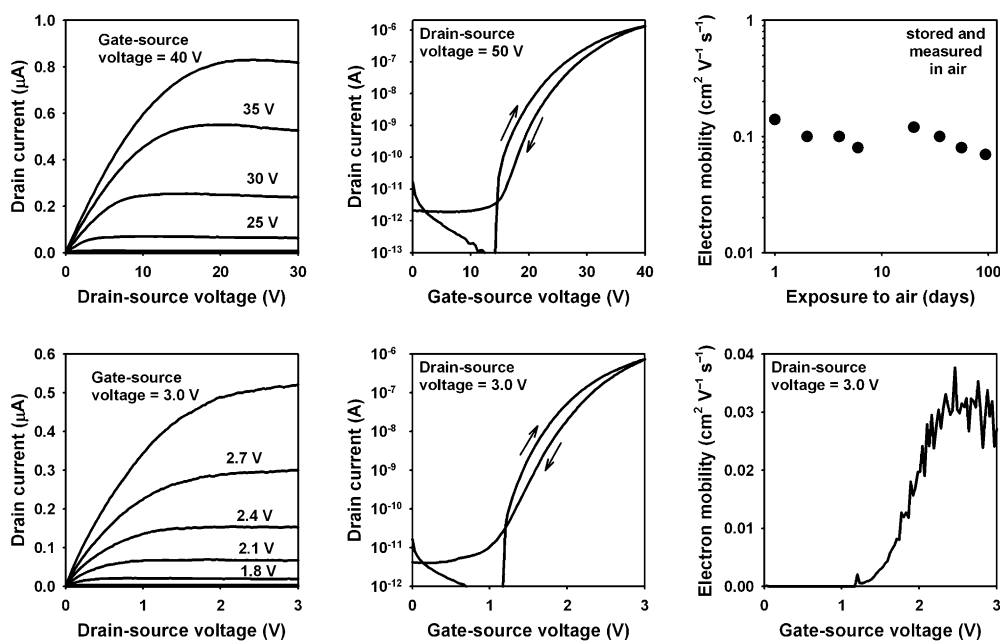


Figure 5. Current–voltage characteristics of TFTs with a vacuum-deposited layer of **8** as the semiconductor. Top: the substrate is a heavily doped Si wafer and the gate dielectric is $\text{SiO}_2/\text{AlO}_x/\text{SAM}$ with a total thickness of 110 nm; bottom: the substrate is glass and the gate dielectric is AlO_x/SAM with a total thickness of 5.3 nm.

carbon atoms, which exhibited a maximum mobility ($\mu_n = 1.2 \text{ cm}^2 \text{V}^{-1} \text{s}^{-1}$ in air) for molecules with heptafluoropropyl substituents connected to the nitrogen atoms of the PTCDI core through a methylene bridge.^[11e]

Comparing the two compounds with the optimum fluororalkyl chain length, **3** (without core substitution) and **8** (with core substitution), it can be seen that the core chlorination provides a higher electron mobility. Since the efficiency of the charge-carrier transport in organic semiconductors is in part determined by the arrangement of the molecules in the solid state,^[27] it is reasonable to consider the parameters obtained from the X-ray analysis of the crystallised compounds (Table 1). The results show that the interplanar distance between neighbouring molecules in the solid-state structures is slightly smaller in the case of **8** (3.38 Å) compared to **3** (3.51 Å). A smaller intermolecular distance, as in the case of **8** compared with **3**, generally leads to better overlap of the π orbitals and thereby to larger carrier mobility.^[28]

Organic complementary circuits: By integrating n- and p-channel TFTs on the same substrate, complementary circuits can be implemented. Compared with unipolar circuits, in which all TFTs conduct the same carrier type, complementary circuits provide several advantages, including larger gain and smaller static power consumption. The schematic representation, a photograph and the transfer characteristics of a complementary inverter with an n-channel TFT based on compound **8** and a p-channel TFT based on dinaphtho-[2,3-b:2',3'-f]thieno[3,2-b]thiophene (DNTT)^[29] fabricated on a glass substrate and patterned using shadow masks are

shown in Figure 6. The inverter has a small-signal gain of about 370 and a static power consumption of about 100 pW.

Figure 7 shows the schematic representation, a photograph and the measured propagation delay per stage as a function of supply voltage of a five-stage complementary ring oscillator fabricated on a glass substrate using n-channel TFTs based on **8** and p-channel TFTs based on DNTT; the TFTs have a channel length of 20 μm .^[30] For comparison, the stage delay of a ring oscillator based on the same layout, but fabricated using hexadecafluorocopperphthalocyanine (F_{16}CuPc) as the semiconductor for the n-channel TFTs is also shown. Compared with F_{16}CuPc , compound **8** provides

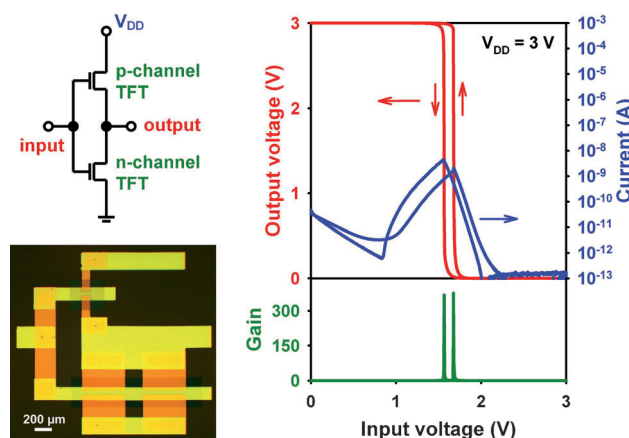


Figure 6. Schematic representation, photograph and transfer characteristics of a complementary inverter with an n-channel TFT based on **8** and a p-channel TFT based on DNTT.

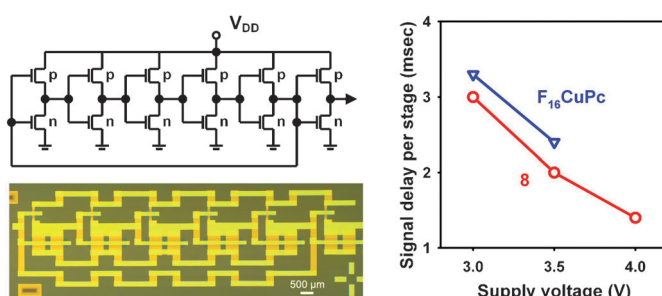


Figure 7. Schematic representation, photograph and signal propagation delay as a function of supply voltage of a 5-stage complementary ring oscillator with n-channel TFTs based on **8** and p-channel TFTs based on DNTT. The TFTs have a channel length of 20 μm . For comparison, the signal delay of a ring oscillator with n-channel TFTs based on hexadecafluorocopperphthalocyanine ($F_{16}\text{CuPc}$) is also shown.

Table 5. Literature summary of the circuit parameters of air-stable organic complementary ring oscillators reported to date.

n-Channel TFT semiconductor	n-Channel TFT mobility [cm^2/Vs]	Ring oscillator operating voltage [V]	Maximum inverter small-signal gain	Minimum ring oscillator signal delay [μs per stage]	Reference
$F_{16}\text{CuPc}$	0.004	100	7	38	[31a]
$F_{16}\text{CuPc}$	0.02	100	4	10	[31b]
$F_{16}\text{CuPc}$	0.002	8–40	6	8	[31c]
$F_{16}\text{CuPc}$	0.02	1.5–3.5	100	2000	[8a]
PTCDI derivative	0.02	100	n/a	45	[31d]
PTCDI derivative	0.001	12	6	740	[31e]
$F_{16}\text{CuPc}$	0.01	1.5–3	40	4500	[31f]
$F_{16}\text{CuPc}$	0.03	1–3	400	1700	[30]
P(NDI2OD-T2)	0.4	20–100	30	2	[31g]
PTVPh1-Eh	0.27	80–160	60	8.3	[31h]
n/a	0.03	40	30	384	[31i]
P(NDI2OD-T2)	0.007	0.2–1.5	18	520	[31j]
$F_{16}\text{CuPc}$	0.02	2	44	110000	[31k]
PTCDI derivative	0.003	100	6	1500	[31l]
$F_{16}\text{CuPc}$	n/a	1–3	30	5600	[31m]
TAPP derivative	0.035	3–4	370	1400	this work

larger electron mobility (0.035 instead of 0.027 $\text{cm}^2\text{V}^{-1}\text{s}^{-1}$) and thus faster circuit speed.^[30] Table 5 provides a literature summary of all air-stable organic complementary ring oscillators and their performance characteristics reported to date.

Conclusion

In this paper we have presented the synthesis and characterisation of a range of 2,9-perfluoroalkyl-substituted tetraazaperopyrene derivatives (**1–5**) and their fourfold core-chlorinated congeners (**6–9**). The optical and electrochemical data demonstrate the drastic influence on the properties that can be achieved by core substitution of TAPPs. In the course of this work we have, for the first time, investigated the performance of TAPP derivatives in organic thin-film transistors. Thereby, we were able to obtain high-performance n-channel transistors with a field-effect mobility of up to

0.14 $\text{cm}^2\text{V}^{-1}\text{s}^{-1}$, an on/off current ratio of $>10^6$ and, above all, remarkable long-term stabilities under ambient conditions of the devices based on compound **8**. These promising results as well as the newly acquired ability to change the substitution pattern of the tetraazaperopyrene not exclusively in the 2- and 9-positions, but also on the central aromatic core, encouraged us to further enhance and improve the properties of this class of compounds with regard to their application as n-type organic semiconductors. Such work is currently under way in our laboratory.

Experimental Section

The syntheses of the 2,9-perfluoroalkyl-substituted tetraazaperopyrenes were performed under dried argon in standard (Schlenk) glassware which was flame dried with a Bunsen burner prior to use. Solvents were dried according to standard procedures and saturated with argon. Solids were separated from suspensions by centrifugation, thus avoiding filtration procedures. The centrifuge employed was a Rotina 48 (Hettich Zentrifugen, Tuttlingen, Germany) which was equipped with a specially designed Schlenk tube rotor.

The ^1H and ^{13}C NMR spectra were recorded by using Bruker AVANCE 400 and 600II⁺ spectrometers equipped with variable-temperature units. Elemental analyses were carried out in the Microanalytical Laboratory of the Chemistry Department at the University of Heidelberg. 4,9-Diamino-3,10-perylenequinone diimine (DPDI) was synthesised as reported previously.^[13] Dichloroisocyanuric acid was supplied by BASF SE. All other starting materials were obtained commercially and used without further purification.

General procedure A for the preparation of the 2,9-disubstituted 1,3,8,10-tetraazaperopyrene (TAPP) derivatives:

Triethylamine (0.4 mL, 2.8 mmol) and the corresponding acid chloride or the acid anhydride (2.5 mmol) were added to a suspension of 4,9-diaminoperylene-quinone-3,10-diimine (DPDI; 310 mg, 1 mmol)^[13] in THF (30 mL), and the mixture was heated to reflux for 72 h. The mixture was allowed to cool to room temperature. The resulting suspension was filtered, washed several times with acetone, ethanol and finally pentane (200 mL). The brown solids were purified by sublimation at 440 °C in a nitrogen stream.

Preparation of 2,9-bis(trifluoromethyl)-1,3,8,10-tetraazaperopyrene (1):

Synthesised according to general procedure A. Acid anhydride: trifluoroacetic anhydride; yield: 280 mg (0.6 mmol; 60%) of **1** as yellow needles; ^1H NMR (399.89 MHz, D_2SO_4 , 300 K): $\delta = 10.44$ (d, $^3J_{\text{HH}} = 9.8$ Hz, 4 H; ^3C H), 9.09 ppm (d, $^3J_{\text{HH}} = 9.1$ Hz, 4 H; ^2C H); ^{13}C NMR (150.90 MHz, $[\text{D}_1]\text{TFA}$, 295 K): $\delta = 154.5$ (C^1), 150.8 (q, $^2J_{\text{CF}} = 41.0$ Hz, C^2), 139.8 (^3C H), 132.3 (C^4), 129.8 (C^2 H), 122.9 (C^5), 120.7 (q, $^1J_{\text{CF}} = 275.3$ Hz, CF_3), 117.8 ppm (C^6); ^{19}F NMR (376.27 MHz, D_2SO_4 , 295 K) $\delta = -66.97$ ppm (s, 6 F; CF_3); HRMS (EI): m/z calcd for $\text{C}_{24}\text{H}_8\text{F}_6\text{N}_4$: 466.0653; found: 466.0645; elemental analysis calcd (%) for $\text{C}_{24}\text{H}_8\text{F}_6\text{N}_4$: C 61.81, H 1.73, N 12.01; found: C 61.97, H 1.85, N 12.04.

Preparation of 2,9-bis(pentafluoroethyl)-1,3,8,10-tetraazaperopyrene (2):

Synthesised according to general procedure A. Acid anhydride: penta-

fluoropropionic anhydride; yield: 360 mg (0.6 mmol; 60%) of **2** as yellow needles; ¹H NMR (600.13 MHz, D₂SO₄, 295 K): δ = 10.71 (d, ³J_{HH} = 10.3 Hz, 4H; C³H), 9.35 ppm (d, ³J_{HH} = 9.1 Hz, 4H; C²H); ¹³C NMR (150.90 MHz, [D₁]TFA, 295 K): δ = 154.4 (C¹), 150.8 (t, ²J_{CF} = 28.7 Hz, C²¹), 140.0 (C³H), 132.4 (C⁴), 129.8 (C²H), 122.8 (C⁵), 118.0 ppm (C⁶); ¹⁹F NMR (376.27 MHz, D₂SO₄, 295 K) δ = -81.6 (m, 6F; CF₃), -117.4 ppm (m, 4F; CF₂); HRMS (FAB⁺): *m/z* calcd for C₂₆H₈F₁₀N₄: 567.0668; found: 567.0664; elemental analysis calcd (%) for C₂₆H₈F₁₀N₄: C 55.14, H 1.42, N 9.89; found C 55.27, H 1.72, N 9.90.

Preparation of 2,9-bis(heptafluoropropyl)-1,3,8,10-tetraazaperopyrene (3): Synthesised according to general procedure A. Acid anhydride: heptafluorobutyric anhydride; yield: 350 mg (0.5 mmol; 53%) of **3** as yellow needles; ¹H NMR (600.13 MHz, D₂SO₄, 295 K): δ = 10.70 (d, ³J_{HH} = 10.1 Hz, 4H; C³H), 9.36 ppm (d, ³J_{HH} = 9.0 Hz, 4H; C²H); ¹³C NMR (150.90 MHz, [D₁]TFA, 295 K): δ = 154.5 (C¹), 150.9 (t, ²J_{CF} = 29.5 Hz, C²¹), 139.9 (C³H), 132.4 (C⁴), 129.9 (C²H), 122.9 (C⁵), 118.0 ppm (C⁶); ¹⁹F NMR (376.27 MHz, D₂SO₄, 295 K) δ = -79.7 (t, ³J_{FF} = 9.1 Hz, 6F; CF₃), -114.6 (m, 4F; CF₂), -124.2 ppm (m, 4F; CF₂); HRMS (FAB⁺): *m/z* calcd for C₂₈H₉F₁₄N₄: 667.0604; found: 667.0611; elemental analysis calcd (%) for C₂₈H₈F₁₄N₄: C 50.47, H 1.21, N 8.41; found: C 50.28, H 1.36, N 8.30.

Preparation of 2,9-bis(nonafluorobutyl)-1,3,8,10-tetraazaperopyrene (4): Synthesised according to general procedure A. Acid chloride: perfluoropentanoyl chloride; yield: 398 mg (0.5 mmol; 52%) of **4** as yellow needles; ¹H NMR (600.13 MHz, D₂SO₄, 295 K): δ = 10.70 (d, ³J_{HH} = 10.2 Hz, 4H; C³H), 9.37 ppm (d, ³J_{HH} = 8.4 Hz, 4H; C²H); ¹³C NMR (150.90 MHz, [D₁]TFA, 295 K): δ = 154.5 (C¹), 151.1 (t, ²J_{CF} = 28.8 Hz, C²¹), 139.9 (C³H), 132.4 (C⁴), 129.9 (C²H), 122.9 (C⁵), 118.0 ppm (C⁶); ¹⁹F NMR (376.27 MHz, D₂SO₄, 295 K) δ = -81.2 (t, ³J_{FF} = 9.3 Hz, 6F; CF₃), -113.9 (m, 4F; CF₂), -120.5 (m, 4F; CF₂), -125.5 ppm (m, 4F; CF₂); HRMS (FAB⁺): *m/z* calcd for C₃₀H₉F₁₈N₄: 767.0540; found: 767.0537; elemental analysis calcd (%) for C₃₀H₈F₁₈N₄: C 47.02, H 1.05, N 7.31; found C 47.23, H 1.32, N 7.48.

Preparation of 2,9-bis(tridecafluorohexanoyl)-1,3,8,10-tetraazaperopyrene (5): Synthesised according to general procedure A. Acid chloride: tridecafluorohexanoyl chloride; yield: 398 mg (0.5 mmol; 52%) of **5** as yellow needles; ¹H NMR (600.13 MHz, D₂SO₄, 295 K): δ = 10.71 (d, ³J_{HH} = 10.2 Hz, 4H; C³H), 9.37 ppm (d, ³J_{HH} = 8.2 Hz, 4H; C²H); ¹³C NMR (150.90 MHz, [D₁]TFA, 295 K): δ = 154.4 (C¹), 151.1 (t, ²J_{CF} = 29.9 Hz, C²¹), 139.9 (C³H), 132.4 (C⁴), 129.9 (C²H), 122.9 (C⁵), 117.9 ppm (C⁶); ¹⁹F NMR (376.27 MHz, D₂SO₄, 295 K) δ = -81.3 (t, ³J_{FF} = 9.8 Hz, 6F; CF₃), -113.7 (m, 4F; CF₂), -119.5 (m, 4F; CF₂), -121.4 (m, 4F; CF₂), -123.0 (m, 4F; CF₂), -126.5 ppm (m, 4F; CF₂); HRMS (FAB⁺): *m/z* calcd for C₃₄H₉F₂₆N₄: 967.0412; found: 967.0430; elemental analysis calcd (%) for C₃₄H₈F₂₆N₄: C 42.26, H 0.83, N 5.80; found: C 42.26, H 0.95, N 5.93.

General procedure B for the chlorination of the 2,9-disubstituted TAPP derivatives: Dichloroisocyanuric acid (280 mg, 1.41 mmol) was added to a solution of the 2,9-disubstituted TAPP derivative (0.25 mmol) in concentrated sulphuric acid (20 mL) and the mixture was stirred at 85 °C for 72 h in the dark. The mixture was allowed to cool to room temperature and then poured in ice water. The resulting precipitate was filtered off and extracted several times with dichloromethane. The solvent was evaporated in vacuum and the resulting red solid recrystallised from THF.

Preparation of 2,9-bis(trifluoromethyl)-4,7,11,14-tetrachloro-1,3,8,10-tetraazaperopyrene (6): Synthesised according to general procedure B. Yield: 85 mg (0.14 mmol; 56%) of **6** as orange needles; ¹H NMR (399.89 MHz, CDCl₃, 295 K): δ = 9.95 ppm (s, 4H; C³H); ¹³C NMR (150.90 MHz, [D₈]THF, 295 K): δ = 159.0 (q, ²J_{CF} = 40.5 Hz, C²¹), 152.9 (C¹), 136.2 (C²Cl), 133.7 (C³H), 128.4 (C⁴), 120.5 (C⁵), 119.4 (C⁶), 116.3 ppm (q, ¹J_{CF} = 286.4 Hz, CF₃); ¹⁹F NMR (376.27 MHz, CDCl₃, 295 K) δ = -68.42 ppm (s, 6F; CF₃); HRMS (EI⁺): *m/z* calcd for C₂₄H₄³⁵Cl₂³⁷Cl₂F₆N₄: 605.9035; found: 605.9010; *m/z* calcd for C₂₄H₄³⁵Cl₃³⁷Cl₂F₆N₄: 603.9065; found: 603.9037; *m/z* calcd for C₂₄H₄³⁵Cl₄F₆N₄: 601.9094; found: 601.9111; elemental analysis calcd (%) for C₂₄H₄F₆Cl₄N₄: C 47.72, H 0.67, N 9.27; found: C 47.32, H 1.02, N 9.45.

Preparation of 2,9-bis(pentafluoroethyl)-4,7,11,14-tetrachloro-1,3,8,10-tetraazaperopyrene (7): Synthesised according to general procedure B. Yield: 155 mg (0.22 mmol; 87%) of **7** as orange needles; ¹H NMR (600.13 MHz, CDCl₃, 295 K): δ = 9.95 ppm (s, 4H; CH); ¹³C NMR (150.90 MHz, [D₈]TFA, 295 K): δ = 156.4–153.4 (m, C²¹), 152.9 (C¹), 136.2 (C²Cl), 133.7 (C³H), 128.4 (C⁴), 120.5 (C⁵), 119.4 ppm (C⁶); ¹⁹F NMR (376.27 MHz, CDCl₃, 295 K) δ = -81.4 (s, 6F; CF₃), -114.9 ppm (s, 4F; CF₂); HRMS (EI⁺): *m/z* calcd for C₂₆H₄³⁵Cl₂³⁷Cl₂F₁₀N₄: 705.8971; found: 705.8959; *m/z* calcd for C₂₆H₄³⁵Cl₃³⁷Cl₂F₁₀N₄: 703.9001; found: 703.8972; *m/z* calcd for C₂₆H₄³⁵Cl₄F₁₀N₄: 701.9030; found: 701.8984; elemental analysis calcd (%) for C₂₆H₄F₁₀Cl₄N₄: C 44.35, H 0.57, N 7.96; found: C 44.21, H 0.57, N 7.96.

Preparation of 2,9-bis(heptafluoropropyl)-4,7,11,14-tetrachloro-1,3,8,10-tetraazaperopyrene (8): Synthesised according to general procedure B. Yield: 137 mg (0.17 mmol; 68%) of **8** as orange needles; ¹H NMR (399.89 MHz, [D₈]THF, 295 K): δ = 10.47 ppm (s, 4H; C³H); ¹³C NMR (150.90 MHz, [D₈]THF, 295 K): δ = 155.5 (t, ²J_{CF} = 25.0 Hz, C²¹), 152.8 (C¹), 136.2 (C²Cl), 133.8 (C³H), 128.5 (C⁴), 120.5 (C⁵), 119.4 ppm (C⁶); ¹⁹F NMR (376.27 MHz, [D₈]THF, 295 K): δ = -80.9 (t, ³J_{FF} = 9.2 Hz, 6F; CF₃), -113.6 (q, ³J_{FF} = 9.1 Hz, 4F; CF₂), -126.0 ppm (m, 4F; CF₂); HRMS (EI): *m/z* calcd for C₂₈H₄³⁵Cl₂³⁷Cl₂F₁₄N₄: 805.8908; found: 805.8933; *m/z* calcd for C₂₈H₄³⁵Cl₃³⁷Cl₂F₁₄N₄: 803.8937; found: 803.8978; *m/z* calcd for C₂₈H₄³⁵Cl₄F₁₄N₄: 801.8967; found: 801.8957; elemental analysis calcd (%) for C₂₈H₄F₁₄Cl₄N₄: C 41.82, H 0.50, N 6.97; found: C 41.56, H 0.95, N 6.94.

Preparation of 2,9-bis(nonafluorobutyl)-4,7,11,14-tetrachloro-1,3,8,10-tetraazaperopyrene (9): Synthesised according to general procedure B. Yield: 99 mg (0.11 mmol; 44%) of **9** as red needles; ¹H NMR (600.13 MHz, [D₈]THF, 295 K): δ = 10.43 ppm (s, 4H; CH); ¹³C NMR (150.90 MHz, [D₈]THF, 295 K): δ = 155.8 (m, C²¹), 152.8 (C¹), 136.2 (C²Cl), 133.8 (C³H), 128.5 (C⁴), 120.5 (C⁵), 119.4 ppm (C⁶); ¹⁹F NMR (376.27 MHz, [D₈]THF, 295 K) δ = -81.8 (m, 6F; CF₃), -112.8 (m, 4F; CF₂), -122.2 (m, 4F; CF₂), -125.9 ppm (m, 4F; CF₂); HRMS (FAB⁺): *m/z* calcd for C₃₀H₅³⁵Cl₂³⁷Cl₂F₁₈N₄: 906.8922; found: 906.8961; *m/z* calcd for C₃₀H₅³⁵Cl₃³⁷ClF₁₈N₄: 904.8951; found: 904.8951; *m/z* calcd for C₃₀H₅³⁵Cl₂F₁₈N₄: 902.8981; found: 902.8964; elemental analysis calcd (%) for C₃₀H₄F₁₈Cl₄N₄: C 39.85, H 0.45, N 6.20; found: C 39.67, H 1.50, N 6.24.

Photophysical measurements: The UV/Vis absorption spectra were recorded on a Cary 5000 UV/Vis/NIR spectrophotometer and were baseline and solvent corrected. Emission spectra were recorded on a Varian Cary Eclipse Spectrophotometer and standard corrections were applied to all spectra. Fluorescence lifetimes were determined on a Fluotime 100 Fluorescence Lifetime System equipped with a PDL 800-D picosecond pulsed Laser unit. The goodness of fit was assessed by minimising the reduced chi-squared function (χ^2) and visual inspection of the weighted residuals. Fluorescence spectra and luminescence quantum yields (Φ_{em}) were measured on a Varian Cary Eclipse Spectrophotometer. Luminescence quantum yields (Φ_{em}) were determined in optically dilute solutions (O.D. < 0.05 at excitation wavelength) and compared to reference emitters by using Equation (1),^[32] in which A is the absorbance at the excitation wavelength (λ), I is the intensity of the excitation light at the excitation wavelength (λ), n is the refractive index of the solvent, D is the integrated intensity of the luminescence and Φ is the quantum yield. The subscripts r and x refer to the reference and the sample, respectively. All quantum yields were performed at identical excitation wavelength for the sample and the reference, canceling the $I(\lambda_r)/I(\lambda_x)$ term in the equation.

$$\Phi_x = \Phi_r \left[\frac{A_r(\lambda_r)}{A_x(\lambda_x)} \right] \left[\frac{I_r(\lambda_r)}{I_x(\lambda_x)} \right] \left[\frac{n_x^2}{n_r^2} \right] \left[\frac{D_x}{D_r} \right] \quad (1)$$

For determining the quantum yields of the discussed samples in THF, either a degassed solution of perylene ($\Phi = 0.94$)^[33] in cyclohexane (**1–5**) or an aqueous solution (0.1 M NaOH) of fluorescein ($\Phi = 0.87$; **6–9**) was used. The solvents for spectroscopic studies were of spectroscopic grade and used as received.

Cyclic voltammetry: Cyclic voltammetry was performed with a standard commercial electrochemical analyser in a three electrode single-compo-

ment cell under argon. A platinum disk was used as the working electrode, a platinum wire as the counter electrode and a saturated calomel electrode as the reference electrode. All potentials were internally referenced to ferrocene. THF was used as solvent that was dried over Na/K and degassed prior to measurement. The supporting electrolyte was 0.1 M tetrabutylammonium hexafluorophosphate. The measurements were carried out under exclusion of air and moisture.

Computational details: The DFT-B3PW91 functional has been employed to model the systems in this work with a 6–31 g(d,p) basis set for all atoms.^[34] All the calculations have been carried out with the GAUSSIAN03 program package.^[35] Every optimisation was followed by a frequency analysis to verify the energy minima. Electron affinities were determined by optimising the structure of the anionic species, using the previously optimised geometry of the neutral species as input and taking the difference of the total energies of both species.

X-ray crystal structure determinations: Crystal data and details of the structure determinations are listed in Table 6. Full shells of intensity data were collected at low temperature (100 K) with a Bruker AXS Smart 1000 CCD diffractometer ($\text{MoK}\alpha$ radiation, graphite monochromator, $\lambda =$

CCDC-844501 (**3**), CCDC-844502 (**7**) and CCDC-844503 (**8**) contain the supplementary crystallographic data for this paper. These data can be obtained free of charge from The Cambridge Crystallographic Data Centre via www.ccdc.cam.ac.uk/data_request/cif.

Acknowledgements

We thank Dr. Dirk-Peter Herten and Arina Rybina for determining the fluorescence lifetimes and Dr. Nicolle Langer (BASF SE, Ludwigshafen) for helpful discussions and provision of the dichloroisocyanuric acid. Financial support from the University of Heidelberg, the Doctoral College “Molekulare Sonden” is gratefully acknowledged. We also thank the German Ministry of Education and Research (BMBF) for funding of this work within the project POLYTOS (FKZ: 13N10205) in the Research Network “Forum Organic Electronics”.

Table 6. Details of the crystal structure determinations of **3**, **7** and **8**.

	3	7	8
formula	$\text{C}_{28}\text{H}_8\text{F}_{14}\text{N}_4$	$\text{C}_{26}\text{H}_4\text{Cl}_4\text{F}_{10}\text{N}_4$	$\text{C}_{28}\text{H}_4\text{Cl}_4\text{F}_{14}\text{N}_4$
M_r	666.38	704.13	804.15
crystal system	triclinic	triclinic	triclinic
space group	$P\bar{1}$	$P\bar{1}$	$P\bar{1}$
a [Å]	4.905(2)	4.945(3)	4.949(3)
b [Å]	9.603(5)	9.477(6)	9.876(6)
c [Å]	13.345(7)	13.060(8)	13.664(7)
α [°]	110.800(8)	82.158(8)	102.988(9)
β [°]	91.275(15)	81.684(9)	95.324(11)
γ [°]	101.904(11)	87.061(17)	91.551(9)
V [Å ³]	571.8(5)	599.6(6)	647.2(6)
Z	1	1	1
F_{000}	330	346	394
ρ_{calcd} [Mg m ⁻³]	1.935	1.950	2.063
$\mu(\text{MoK}\alpha)$ [mm ⁻¹]	0.197	0.602	0.593
max/min transmission	0.8623/0.7806	1.0000/0.7986	0.74633/0.65680
θ range [°]	2.3–27.9	2.2–27.1	2.1–32.0
index ranges	$-6 \leq h \leq 6$ $-12 \leq k \leq 11$ $0 \leq l \leq 17$	$-6 \leq h \leq 6$ $-11 \leq k \leq 12$ $0 \leq l \leq 16$	$-7 \leq h \leq 7$ $-14 \leq k \leq 14$ $0 \leq l \leq 20$
reflections measured	11120	10314	25622
unique $[R_{\text{int}}]$	2727 [0.0452]	2633 [0.0526]	4169 [0.0545]
observed [$I \geq 2\sigma(I)$]	1739	1902	3171
parameters refined	220	199	226
GooF on F^2	1.006	1.028	1.063
R indices [$F > 4\sigma(F)$] $R(F)$, $wR(F^2)$	0.0457, 0.1063	0.0515, 0.1306	0.0532, 0.1303
R indices (all data) $R(F)$, $wR(F^2)$	0.0897, 0.1263	0.0804, 0.1445	0.0731, 0.1377
largest residual peaks [e Å ⁻³]	0.423, -0.306	0.530, -0.518	0.705, -0.660

0.71073 Å). Data were corrected for air and detector absorption, Lorentz and polarisation effects;^[36] absorption by the crystal was treated numerically or with a semiempirical multiscan method.^[37–39] The structures were solved by conventional direct methods^[40,41] or by the charge flip procedure^[42] and refined by full-matrix least-squares methods based on F^2 against all unique reflections.^[41,43] All non-hydrogen atoms were given anisotropic displacement parameters. Hydrogen atoms were generally placed at calculated positions and refined with a riding model. When justified by the quality of the data the positions of some hydrogen atoms (compound **3**) were taken from difference Fourier syntheses and refined. Crystals of compound **8** were twinned. Data were collected from a specimen with 0.84:0.16 twin fractions. Only singles and composites that included the larger domain were used for refinement.

- [1] a) K. Müllen, U. Scherf (Eds.), in *Organic Light Emitting Devices, Synthesis Properties and Applications*, Wiley-VCH, Weinheim, Germany, **2005**; b) H. Klauk, in *Organic Electronics*, Wiley-VCH, Weinheim, **2006**.
- [2] For recent reviews on this subject see: a) J. Zaumseil, H. Sirringhaus, *Chem. Rev.* **2007**, *107*, 1296–1323; b) S. Allard, M. Forster, B. Souharce, H. Thiem, U. Scherf, *Angew. Chem.* **2008**, *120*, 4138–4167; *Angew. Chem. Int. Ed.* **2008**, *47*, 4070–4098; c) H. E. Katz, J. Huang, *Annu. Rev. Mater. Res.* **2009**, *39*, 71–92; d) D. Braga, G. Horowitz, *Adv. Mater.* **2009**, *21*, 1473–1486; e) H. Usta, C. Risko, Z. Wang, H. Huang, M. K. Deliomeroglu, A. Zhukhovitskiy, A. Faccetti, T. J. Marks, *J. Am. Chem. Soc.* **2009**, *131*, 5586–5608; f) F. Würthner, K. Meerholz, *Chem. Eur. J.* **2010**, *16*, 9366–9373.
- [3] See for example: a) L. Schmidt-Mende, A. Fechtenköter, K. Müllen, E. Moons, R. H. Friend, J. D. MacKenzie, *Science* **2001**, *293*, 1119–1122; b) C. R. Newman, C. D. Frisbie, D. A. da Silva Filho, J.-L. Brédas, P. C. Ewbank, K. R. Mann, *Chem. Mater.* **2004**, *16*, 4436–4451; c) M. M. Ling, Z. Bao, *Chem. Mater.* **2004**, *16*, 4824–4840; d) W. Pisula, A. Menon, M. Stepputat, I. Lieberwirth, U. Kolb, A. Tracz, H. Sirringhaus, T. Pakula, K. Müllen, *Adv. Mater.* **2005**, *17*, 684–689; e) F. Würthner, R. Schmidt, *ChemPhysChem* **2006**, *7*, 793–797; f) Z. Chen, V. Stepanenko, V. Dehm, P. Prins, L. D. A. Siebbeles, J. Seibt, P. Marquetand, V. Engel, F. Würthner, *Chem. Eur. J.* **2007**, *13*, 436–449; g) X. Guo, R. P. Ortiz, Y. Zheng, Y. Hu, Y.-Y. Noh, K.-J. Baeg, A. Faccetti, T. J. Marks, *J. Am. Chem. Soc.* **2011**, *133*, 1405–1418.
- [4] a) F. Würthner, *Angew. Chem.* **2001**, *113*, 1069–1071; *Angew. Chem. Int. Ed.* **2001**, *40*, 1037–1039; b) J. E. Anthony, *Chem. Rev.* **2006**, *106*, 5028–5048; c) X. Feng, W. Pisula, K. Müllen, *Pure Appl. Chem.* **2009**, *81*, 2203–2224; d) D. S. Weiss, M. Abkowitz, *Chem. Rev.* **2010**,

- 110, 479–526; e) A. W. Hains, Z. Liang, M. A. Woodhouse, B. A. Gregg, *Chem. Rev.* **2010**, *110*, 6689–6735.
- [5] H. Klauk, *Chem. Soc. Rev.* **2010**, *39*, 2643–2666.
- [6] a) X. Zhan, A. Facchetti, S. Barlow, T. J. Marks, M. A. Ratner, M. R. Wasielewski, S. R. Marder, *Adv. Mater.* **2011**, *23*, 268–284; b) H. Usta, A. Facchetti, T. J. Marks, *Acc. Chem. Res.* **2011**, *44*, 501–510.
- [7] a) M. Halik, H. Klauk, U. Zschieschang, G. Schmid, S. Ponomarenko, S. Kirchmeyer, W. Weber, *Adv. Mater.* **2003**, *15*, 917–922; b) J. E. Anthony, *Angew. Chem.* **2008**, *120*, 460–492; *Angew. Chem. Int. Ed.* **2008**, *47*, 452–483; c) M. L. Tang, A. D. Reichhardt, T. Siegrist, S. C. B. Mannsfeld, Z. Bao, *Chem. Mater.* **2008**, *20*, 4669–4676; d) S. Subramanian, S. K. Park, S. R. Parkin, V. Podzorov, T. N. Jackson, J. E. Anthony, *J. Am. Chem. Soc.* **2008**, *130*, 2706–2707; e) P. Gao, D. Beckmann, H. N. Tsao, X. Feng, V. Enkelmann, M. Baumgarten, W. Pisula, K. Müllen, *Adv. Mater.* **2009**, *21*, 213–216.
- [8] a) H. Klauk, U. Zschieschang, J. Pflaum, M. Halik, *Nature* **2007**, *445*, 745–748; b) T. Fujimoto, Y. Miyoshi, M. M. Matsushita, K. Awaga, *Chem. Commun.* **2011**, *47*, 5837–5839.
- [9] a) C. J. Tonzola, M. M. Alam, W. Kaminsky, S. A. Jenekhe, *J. Am. Chem. Soc.* **2003**, *125*, 13548–13558; b) M. J. D. Bosdet, W. E. Piers, Ted. S. Sorensen, M. Parvez, *Angew. Chem.* **2007**, *119*, 5028–5031; *Angew. Chem. Int. Ed.* **2007**, *46*, 4940–4943; c) M. Takase, V. Enkelmann, D. Sebastiani, M. Baumgarten, K. Müllen, *Angew. Chem.* **2007**, *119*, 5620–5623; *Angew. Chem. Int. Ed.* **2007**, *46*, 5524–5527; d) S. Alibert-Fouet, I. Seguy, J.-F. Bobo, P. Destruel, H. Bock, *Chem. Eur. J.* **2007**, *13*, 1746–1753; e) F. Würthner, M. Stolte, *Chem. Commun.* **2011**, *47*, 5109–5115.
- [10] a) R. T. Weitz, K. Amsharov, U. Zschieschang, E. B. Villas, D. K. Goswami, M. Burghard, H. Dosch, M. Jansen, K. Kern, H. Klauk, *J. Am. Chem. Soc.* **2008**, *130*, 4637–4645; b) U. Zschieschang, K. Amsharov, R. T. Weitz, M. Jansen, H. Klauk, *Synth. Met.* **2009**, *159*, 2362–2364.
- [11] a) Z. Bao, A. Lovinger, J. Brown, *J. Am. Chem. Soc.* **1998**, *120*, 207–208; b) H. E. Katz, J. Johnson, A. J. Lovinger, W. Li, *J. Am. Chem. Soc.* **2000**, *122*, 7787–7792; c) B. A. Jones, M. J. Ahrens, M. H. Yoon, A. Facchetti, T. J. Marks, M. R. Wasielewski, *Angew. Chem.* **2004**, *116*, 6523–6526; *Angew. Chem. Int. Ed.* **2004**, *43*, 6363–6366; d) H. Z. Chen, M. M. Ling, X. Mo, M. M. Shi, M. Wang, Z. Bao, *Chem. Mater.* **2007**, *19*, 816–824; e) R. Schmidt, J. H. Oh, Y.-S. Sun, M. Deppisch, A.-M. Krause, K. Radacki, H. Braunschweig, M. Könemann, P. Erk, Z. Bao, F. Würthner, *J. Am. Chem. Soc.* **2009**, *131*, 6215–6228; f) J. H. Oh, S. L. Suraru, W. Y. Lee, M. Könemann, H. W. Höffken, C. Röger, R. Schmidt, Y. Chung, W. C. Chen, F. Würthner, Z. Bao, *Adv. Funct. Mater.* **2010**, *20*, 2148–2156.
- [12] M. Gsänger, J. H. Oh, M. Könemann, H. W. Höffken, A.-M. Krause, Z. Bao, F. Würthner, *Angew. Chem.* **2010**, *122*, 752–755; *Angew. Chem. Int. Ed.* **2010**, *49*, 740–743.
- [13] a) K. W. Hellmann, C. H. Galka, I. Rüdenauer, L. H. Gade, I. J. Scowen, M. McPartlin, *Angew. Chem.* **1998**, *110*, 2053–2057; *Angew. Chem. Int. Ed.* **1998**, *37*, 1948–1952; b) L. H. Gade, C. H. Galka, K. W. Hellmann, R. M. Williams, L. De Cola, I. J. Scowen, M. McPartlin, *Chem. Eur. J.* **2002**, *8*, 3732–3746; c) L. H. Gade, C. H. Galka, R. M. Williams, L. De Cola, M. McPartlin, L. Chi, B. Dong, *Angew. Chem.* **2003**, *115*, 2781–2785; *Angew. Chem. Int. Ed.* **2003**, *42*, 2677–2681.
- [14] a) M. Stöhr, M. Wahl, C. H. Galka, T. Riehm, T. A. Jung, L. H. Gade, *Angew. Chem.* **2005**, *117*, 7560–7564; *Angew. Chem. Int. Ed.* **2005**, *44*, 7394–7398; b) M. Wahl, M. Stöhr, H. Spillmann, T. A. Jung, L. H. Gade, *Chem. Commun.* **2007**, 1349–1351; c) M. Stöhr, M. Wahl, H. Spillmann, L. H. Gade, T. A. Jung, *Small* **2007**, *3*, 1336–1340; d) J. Lobo-Checa, M. Matena, K. Müller, J. H. Dil, F. Meier, L. H. Gade, T. A. Jung, M. Stöhr, *Science* **2009**, *325*, 300–303.
- [15] T. Riehm, G. De Paoli, A. E. Konradsson, L. De Cola, H. Wade, L. H. Gade, *Chem. Eur. J.* **2007**, *13*, 7317–7329.
- [16] a) M. Matena, T. Riehm, M. Stöhr, T. A. Jung, L. H. Gade, *Angew. Chem.* **2008**, *120*, 2448–2451; *Angew. Chem. Int. Ed.* **2008**, *47*, 2414–2417; b) M. Matena, M. Stöhr, T. Riehm, J. Björk, S. Martens, M. S. Dyer, M. Persson, J. Lobo-Checa, K. Müller, M. Enache, H. Wade, pohl, J. Zegenhagen, T. A. Jung, L. H. Gade, *Chem. Eur. J.* **2010**, *16*, 2079–2091; c) J. Björk, M. Matena, M. S. Dyer, M. Enache, J. Lobo-Checa, L. H. Gade, T. A. Jung, M. Stöhr, M. Persson, *Phys. Chem. Chem. Phys.* **2010**, *12*, 8815–8821.
- [17] B. A. Jones, A. Facchetti, M. R. Wasielewski, T. J. Marks, *J. Am. Chem. Soc.* **2007**, *129*, 15259–15278.
- [18] a) H. E. Katz, A. J. Lovinger, J. Johnson, C. Kloc, T. Siegrist, W. Li, Y.-Y. Lin, A. Dodabalapur, *Nature* **2000**, *404*, 478–481; b) H. E. Katz, T. Siegrist, J. H. Schön, C. Kloc, B. Batlogg, A. J. Lovinger, J. Johnson, *ChemPhysChem* **2001**, *2*, 167–172; c) C. D. Dimitrakopoulos, P. R. Malenfant, *Adv. Mater.* **2002**, *14*, 99–117.
- [19] G. Klebe, F. Graser, E. Hädicke, J. Berndt, *Acta Crystallogr. Sect. B* **1989**, *45*, 69–77.
- [20] S. C. Martens, T. Riehm, S. Geib, H. Wade, L. H. Gade, *J. Org. Chem.* **2011**, *76*, 609–617.
- [21] See for example: a) M.-M. Ling, P. Erk, M. Gomez, M. Könemann, J. Locklin, Z. Bao, *Adv. Mater.* **2007**, *19*, 1123–1127; b) R. Schmidt, M.-M. Ling, J. H. Oh, M. Winkler, M. Könemann, Z. Bao, F. Würthner, *Adv. Mater.* **2007**, *19*, 3692–3695.
- [22] I. Seguy, P. Jolinat, P. Destruel, R. Mamy, H. Allouchi, C. Courseille, M. Cotrait, H. Bock, *ChemPhysChem* **2001**, *2*, 448–458.
- [23] For analytical data of this compound see Supporting Information.
- [24] Y.-C. Chang, M.-Y. Kuo, C.-P. Chen, H.-F. Lu, I. Chao, *J. Phys. Chem. C* **2010**, *114*, 11595–11601.
- [25] H. Y. Nie, *Anal. Chem.* **2010**, *82*, 3371–3376.
- [26] S. M. Sze, in *Semiconductor Devices*, Wiley, New York, **1985**.
- [27] a) B. Servet, G. Horowitz, S. Ries, O. Lagorse, P. Alnot, A. Yassar, F. Deloffre, P. Srivastava, P. Hajlaoui, P. Lang, F. Garnier, *Chem. Mater.* **1994**, *6*, 1809–1815; b) J. Locklin, D. Li, S. C. B. Mannsfeld, E.-J. Borkent, H. Meng, R. Advincula, Z. Bao, *Chem. Mater.* **2005**, *17*, 3366–3374.
- [28] J. Cornil, D. Beljonne, J. P. Calbert, J. L. Bredas, *Adv. Mater.* **2001**, *13*, 1053–1067.
- [29] U. Zschieschang, F. Ante, D. Käblein, T. Yamamoto, K. Takimiya, H. Kuwabara, M. Ikeda, T. Sekitani, T. Someya, J. Blochwitz-Nimoth, H. Klauk, *Org. Electron.* **2011**, *12*, 1370–1375.
- [30] U. Zschieschang, F. Ante, M. Schlörholz, M. Schmidt, K. Kern, H. Klauk, *Adv. Mater.* **2010**, *22*, 4489–4493.
- [31] a) Y. Y. Lin, A. Dodabalapur, R. Sarapeshkar, Z. Bao, W. Li, K. Baldwin, V. R. Raju, H. E. Katz, *Appl. Phys. Lett.* **1999**, *74*, 2714–2716; b) B. K. Crone, A. Dodabalapur, R. Sarapeshkar, R. W. Filas, Y. Y. Lin, Z. Bao, J. H. O'Neill, W. Li, H. E. Katz, *J. Appl. Phys.* **2001**, *89*, 5125–5132; c) H. Klauk, M. Halik, U. Zschieschang, F. Eder, D. Rohde, G. Schmid, C. Dehm, *IEEE Trans. Electron Devices* **2005**, *52*, 618–622; d) B. Yoo, B. A. Jones, D. Basu, D. Fine, T. Jung, S. Mohapatra, A. Facchetti, K. Dimmler, M. R. Wasielewski, T. J. Marks, A. Dodabalapur, *Adv. Mater.* **2007**, *19*, 4028–4032; e) H. Yan, Y. Zheng, R. Blache, C. Newman, S. Lu, J. Woerle, A. Facchetti, *Adv. Mater.* **2008**, *20*, 3393–3398; f) T. Sekitani, U. Zschieschang, H. Klauk, T. Someya, *Nat. Mater.* **2010**, *9*, 1015–1022; g) K. J. Baeg, D. Khim, D. Y. Kim, S. W. Jung, J. B. Koo, I. K. You, H. Yan, A. Facchetti, Y. Y. Noh, *J. Polym. Sci. Part B: Polym. Phys.* **2011**, *49*, 62–67; h) K. J. Baeg, J. Kim, D. Khim, M. Caironi, D. Y. Kim, I. K. You, J. R. Quinn, A. Facchetti, Y. Y. Noh, *ACS Appl. Mater. Interfaces* **2011**, *3*, 3205–3214; i) M. Guerin, A. Daami, S. Jacob, E. Bergeret, E. Benevent, P. Pannier, R. Coppard, *IEEE Trans. Electron Devices* **2011**, *58*, 3587–3593; j) L. Herlogsson, X. Crispin, S. Tiemey, M. Berggren, *Adv. Mater.* **2011**, *23*, 4684–4689; k) K. Ishida, N. Masunaga, R. Takahashi, T. Sekitani, S. Shino, U. Zschieschang, H. Klauk, M. Takamiya, T. Someya, T. Sakurai, *IEEE J. Solid-State Circuits* **2011**, *46*, 285–292; l) H. Kempa, M. Hamsch, K. Reuter, M. Stanel, G. C. Schmidt, B. Meier, A. C. Hübler, *IEEE Trans. Electron Devices* **2011**, *58*, 2765–2769; m) T. Yokota, T. Nakagawa, T. Sekitani, Y. Noguchi, K. Fukuda, U. Zschieschang, H. Klauk, K. Takeuchi, M. Takamiya, T. Sakurai, T. Someya, *Appl. Phys. Lett.* **2011**, *98*, 193302/1–3.
- [32] D. F. Eaton, *Pure Appl. Chem.* **1988**, *60*, 1107–1114.
- [33] I. B. Berlman, in *Handbook of Fluorescence Spectra of Aromatic Molecules*, Academic Press, New York, **1965**.

- [34] a) W. J. Hehre, R. Ditchfield, J. A. Pople, *J. Chem. Phys.* **1972**, *56*, 2257–2261; b) j. D. Dill, J. A. Pople, *J. Chem. Phys.* **1975**, *62*, 2921–2923; c) M. M. Francz, W. J. Pietro, W. J. Hehre, J. S. Binkley, M. S. Gordon, D. J. DeFrees, J. A. Pople, *J. Chem. Phys.* **1982**, *77*, 3654–3665; d) T. Clark, J. Chandrasekhar, G. W. Spitznagel, P. V. R. Schleyer, *J. Comput. Chem.* **1983**, *4*, 294–301.
- [35] Gaussian 03, Version D.02, M. J. Frisch, G. W. Trucks, H. B. Schlegel, G. E. Scuseria, M. A. Robb, J. R. Cheeseman, J. A. Montgomery, Jr., T. Vreven, K. N. Kudin, J. C. Burant, J. M. Millam, S. S. Iyengar, J. Tomasi, V. Barone, B. Mennucci, M. Cossi, G. Scalmani, N. Rega, G. A. Petersson, H. Nakatsuji, M. Hada, M. Ehara, K. Toyota, R. Fukuda, J. Hasegawa, M. Ishida, T. Nakajima, Y. Honda, O. Kitao, H. Nakai, M. Klene, X. Li, J. E. Knox, H. P. Hratchian, J. B. Cross, V. Bakken, C. Adamo, J. Jaramillo, R. Gomperts, R. E. Stratmann, O. Yazyev, A. J. Austin, R. Cammi, C. Pomelli, J. W. Ochterski, P. Y. Ayala, K. Morokuma, G. A. Voth, P. Salvador, J. J. Dannenberg, V. G. Zakrzewski, S. Dapprich, A. D. Daniels, M. C. Strain, O. Farkas, D. K. Malick, A. D. Rabuck, K. Raghavachari, J. B. Foresman, J. V. Ortiz, Q. Cui, A. G. Baboul, S. Clifford, J. Cioslowski, B. B. Stefanov, G. Liu, A. Liashenko, P. Piskorz, I. Komaromi, R. L. Martin, D. J. Fox, T. Keith, M. A. Al-Laham, C. Y. Peng, A. Nanayakkara, M. Challacombe, P. M. W. Gill, B. Johnson, W. Chen, M. W. Wong, C. Gonzalez, J. A. Pople, Gaussian, Inc., Wallingford, CT, **2004**.
- [36] SAINT, Bruker AXS, **1997–2008**.
- [37] R. H. Blessing, *Acta Crystallogr. Sect. A* **1995**, *51*, 33–38.
- [38] G. M. Sheldrick, SADABS, Bruker AXS, **2004–2008**.
- [39] G. M. Sheldrick, TWINABS, Bruker AXS, **2008**.
- [40] G. M. Sheldrick, SHELXS-97, University of Göttingen, Germany, **1997**.
- [41] G. M. Sheldrick, *Acta Crystallogr. Sect. A* **2008**, *64*, 112.
- [42] a) L. Palatinus, SUPERFLIP, EPFL Lausanne, Switzerland, **2007**; b) L. Palatinus, G. Chapuis, *J. Appl. Crystallogr.* **2007**, *40*, 786–790.
- [43] G. M. Sheldrick, SHELXL-97, University of Göttingen, **1997**.

Received: October 7, 2011
Published online: February 22, 2012

CHEMISTRY

A EUROPEAN JOURNAL

Supporting Information

© Copyright Wiley-VCH Verlag GmbH & Co. KGaA, 69451 Weinheim, 2012

Tetrachlorinated Tetraazaperopyrenes (TAPPs): Highly Fluorescent Dyes and Semiconductors for Air-Stable Organic n-Channel Transistors and Complementary Circuits

**Susanne C. Martens,^[a] Ute Zschieschang,^[b] Hubert Wadepohl,^[a] Hagen Klauk,^[b] and
Lutz H. Gade^{*[a]}**

chem_201103158_sm_miscellaneous_information.pdf

Supporting Information for

**Tetrachlorinated Tetraazaperopyrenes (TAPPs): Highly Fluorescent Dyes and
Semiconductors for Air-Stable Organic n-Channel Transistors and Complementary
Circuits**

**Susanne C. Martens^[a] Ute Zschieschang,^[b] Hubert Wadeohl,^[a] Hagen Klauk^[b]
and Lutz H. Gade^{*[a]}**

*[a] Anorganisch-Chemisches Institut, Universität Heidelberg, Im Neuenheimer Feld 270,
69120 Heidelberg, Germany*

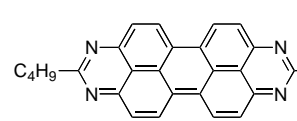
[b] Max Planck Institute for Solid Research, Heisenbergstr. 1, 70569 Stuttgart, Germany

E-Mail: Lutz.Gade@uni-hd.de

Contents:

SI.1 Synthesis and Analytical Data of 2,9-Di-<i>n</i>-butyl-1,3,8,10-tetraazaperopyrene	2
SI.2 References	2

SI.1 Synthesis and Analytical Data of 2,9-di-n-butyl-1,3,8,10-tetraaza peropyrene



To a suspension of 310 mg (1 mmol) 4,9-diaminoperylene-quinone-3,10-diimine (DPDI)^[SI1] in 30 ml THF 0.4 ml (2.8 mmol) triethylamine and 0.3 ml (2.5 mmol) of pentanoyl chloride were added, and the mixture was heated to reflux for 72 h. The mixture was allowed to cool to room temperature. The resulting suspension was filtered, washed several times with acetone, ethanol and finally pentane (200 ml). The brown solids were purified by sublimation at 440 °C in a nitrogen stream.

¹H NMR (399.89 MHz, [D₁]TFA, 300 K): δ = 10.42 (d, 4H, ³J = 9.5 Hz, C³H), 9.11 ppm (d, 4H, ³J = 9.5 Hz, C²H), 3.67 ppm, (t, 6H, ³J_{HH} = 7.9 Hz, CH₂), 2.16 (quint, 4H, ³J_{HH} = 7.4 Hz, CH₂), 1.60 (sext, 4H, ³J_{HH} = 7.4 Hz, CH₂), 1.02 (t, 6H, ³J_{HH} = 7.3 Hz, CH₃); ¹³C NMR (150.90 MHz, [D₁]TFA, 295 K): δ = 166.6 (C²¹), 153.6 (C¹), 140.5 (C³), 131.9 (C⁴H), 128.0 (C²H), 122.7 (C⁵), 116.1 (C⁶), 38.2 (CH₂), 33.1 (CH₂), 24.3 (CH₂), 14.0 (CH₃); HRMS (FAB⁺) *m/z* calcd for C₃₀H₂₇N₄: 443.2236; found: 443.2257; elemental analysis calcd (%) for C₃₀H₂₆N₄: C 81.42, H 5.92, N 12.66; found: C 81.73, H 6.00, N 12.43.

Cyclic voltammetry data measured in THF: E_{red1} = -0.84 V; E_{red2} = -1.23 V.

E_{LUMO}(CV)^[SI2] = -3.38 V.

EA (calculated at the B3PW91/6-31g(d,p) level of theory) = 2.37 V.

SI.2 References:

- [SI1] a) K. W. Hellmann, C. H. Galka, I. Rüdenauer, L. H. Gade, I. J. Scowen, M. McPartlin, *Angew. Chem.* **1998**, *110*, 2053-2057; *Angew Chem. Int. Ed.* **1998**, *37*, 1948-1952; b) L. H. Gade, C. H. Galka, K. W. Hellmann, R. M. Williams, L. De Cola, I. J. Scowen, M. McPartlin, *Chem. Eur. J.* **2002**, *8*, 3732-3746; c) L. H. Gade, C. H. Galka, R. M. Williams, L. De Cola, M. McPartlin, L. Chi, B. Dong, *Angew. Chem.* **2003**, *115*, 2781-2785; *Angew. Chem. Int. Ed.* **2003**, *42*, 2677-2681.
- [SI2] I. Seguy, P. Jolinat, P. Destruel, R. Mamy, H. Allouchi, C. Courseille, M. Cotrait, H. Bock, *ChemPhysChem*, **2001**, *2*, 448-452.